Micromachined Multimode Interference Device in Flat-fiber

S. Ambran[1,2], C. Holmes[1], J.C. Gates[1], A.S. Webb[1], F.R. Mahamd Adikan[3], P.G.R. Smith[1], J.K. Sahu[1]
1) Optoelectronics Research Centre (ORC), University of Southampton, United Kingdom
2) University Technology of Malaysia, Malaysia
3) University of Malaya, Malaysia
sa4g09@orc.soton.ac.uk

***Abstract*- We demonstrate a new approach for fabricating multimode interference (MMI) devices using micromachining of a novel flat-fiber platform. A 1x3 splitter has been demonstrated together with spatial output mode control by index tuning of material within micromachined trenches.**

I. INTRODUCTION

Multimode Interference (MMI) has been demonstrated as a powerful technique for many applications in integrated optics [1]. It offers small device size, polarization insensitivity, stable power splitting ratios and temperature insensitivity. However, it has not yet found widespread application due to the cost of fabrication and the difficulty in implementing devices in a low index contrast material system such as silica-on-silicon, where dopant levels typically limit index contrast to less than 1%. Recently, the use of air channels has been suggested as it offers the potential of reduced insertion loss by significantly increasing the lateral index contrast [2].

Self-imaging is a key concept for MMI device operation by which the input field is reproduced as single or multiple images at the end face of the MMI structure. It has been extensively observed in different geometries particularly in planar and circular shapes [3]. MMI devices have been demonstrated in different planar material systems such as crystals [4], Flame Hydrolysis Deposited (FHD) silica-on-silicon substrates [5], Sol-Gel hybrid [6] and polymer [7]. However, many of these materials are potentially expensive, rigid, high loss or have complex fabrication processes.

The desire to have a fiber-like platform, capable of supporting multiple waveguides in a planar format, has led the group of Southampton to develop a novel silica optical flat-fiber technology [8]. This platform can overcomes the limitations of existing planar technologies by offering a low cost fabrication process; low loss substrates with fiber-like flexibility; long lengths and the ability to make integrated devices. The flat-fiber is fabricated using existing fiber fabrication equipment leading to an economical and uncomplicated fabrication process. Fig. 1 shows the end-facet and the bending of a length of flat-fiber illustrating its geometry.

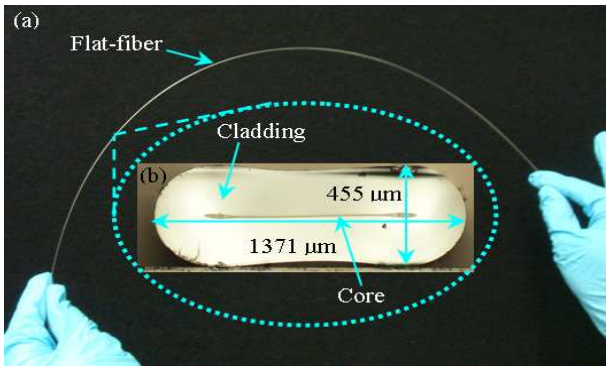

Fig. 1. (a) Bending and (b) Cross section of flat-fiber

In this paper, we used a flat-fiber substrate which is made from standard fiber-type MCVD (Modified Chemical Vapor Deposition) silica layers that are flattened and drawn to create the final substrate. The process differs from standard fiber production in that the collapsing of the preform during the fiber drawing stage uses a vacuum to obtain a flattened structure. It can be seen from Fig. 1 that the flat-fiber has a planar core layer which is used for light guidance. Here, for the first time, micromachined MMI devices in the flat-fiber substrate are presented, and specifically a 1x3 power splitter is demonstrated as shown schematically in Fig. 2. A Fast-Fourier Transform Beam Propagation Method (FFT-BPM) was used in order to understand the operation of the MMI light propagation along the waveguide region.

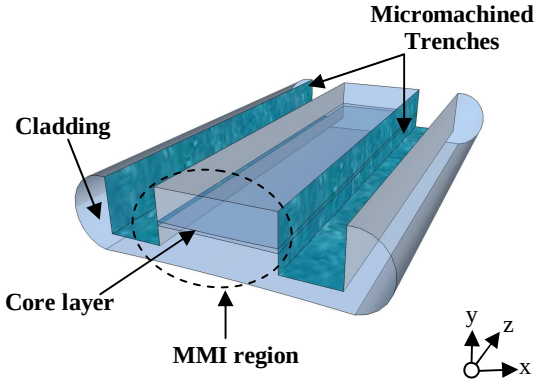

Fig. 2. A 3-D schematic of the air-trenches MMI flat-fiber

II. CONCEPT AND THEORY

Fig. 3 shows a schematic of the flat-fiber MMI structure. There are two micromachined trenches in parallel with the MMI region, which limits the width of the MMI region and offers shorter self-imaging length and hence shorter devices. The trenches were cut using an ultra-precision dicing saw.

The self-imaging operation of an MMI device primarily depends on three parameters, the effective width, W_{eff}, the effective refractive index, n_{eff} and the operation wavelength, λ. The self-imaging length is given by (1) [9].

$$L_{MMI} = \frac{n_{eff}(W_{eff})^2}{\lambda} \qquad (1)$$

As well as providing lateral confinement, the use of trenches allows us to add refractive index oils into the trench and exposes the core layer to different refractive index values. This will affect the effective width of the MMI region due to the Goos-Hänchen effect that results in the light penetrating into the cladding region of the MMI. As a result, different mode profiles will be generated due to the different index contrast of the cladding region in the trenches.

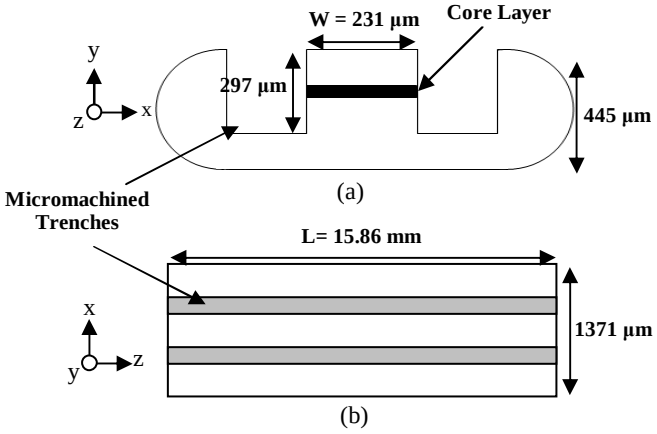

Fig. 3. A schematic diagram of MMI flat-fiber (a) End face view and (b) top-view.

III. RESULT AND DISCUSSIONS

In order to predict the operation of the micromachined trenches MMI device, we used FFT-BPM as depicted in Fig. 4(a). By selecting an appropriate length, a clear pattern of three output modes is revealed in Fig. 4(b). Fig. 4(c) shows a simulation of the device output pattern with the same parameters as in Fig. 4(b), but with index oil of 1.44 added to the trenches. Note the formation of additional fine-scale features in the output mode. The simulation result has been convoluted with a Gaussian profile representing the SMF-28 fiber accordingly.

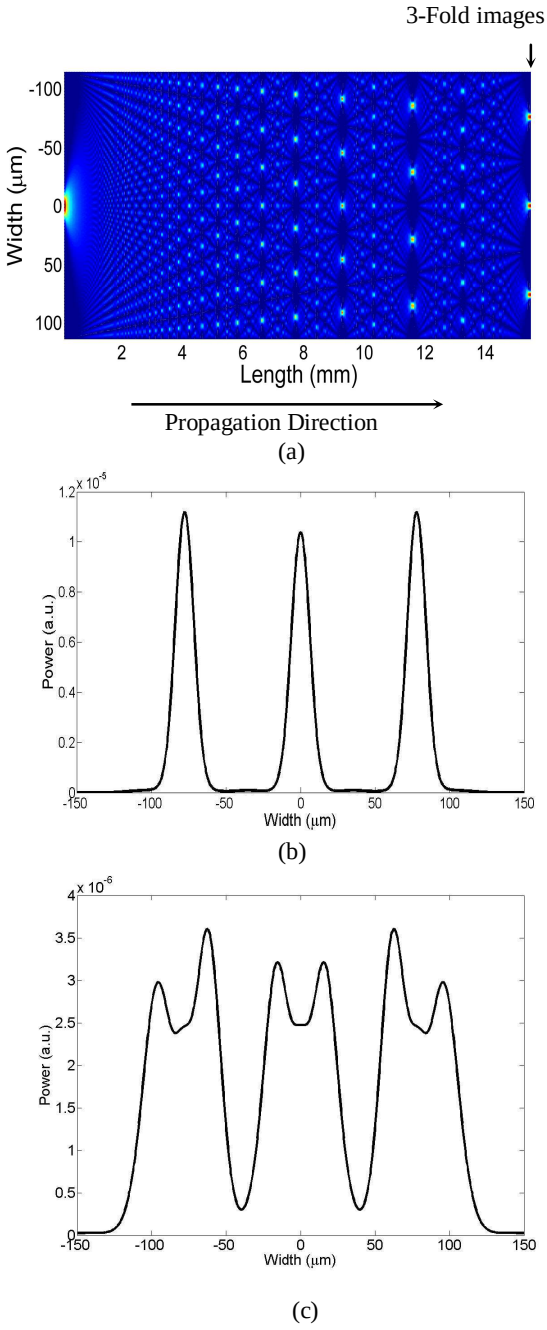

Fig. 4. BPM simulation for the MMI region (Width = 231 µm) (a) Beam propagation pattern (top-view), (b) Mode profile at the output facet and (c) Simulation at the 3-fold image plane (L=15.86 mm) when using index oil of 1.44 in the trenches.

Experimentally, the MMI device was characterized using a polarized tunable light source and launched into the middle of the MMI region using a single mode fiber (SMF-28). Beforehand, the light was adjusted to have Transverse Magnetic (TM) polarization by using a polarization controller. The characterization setup is shown in Fig. 5. The output facet image was observed by using a near infrared (NIR) camera. In order to measure the intensity of each output spot, we used a scanning technique at the end-

facet of the MMI region to overcome the small dynamic range of the NIR camera. Therefore, the output facet of the MMI region was scanned by using a SM fiber and measured with a power meter.

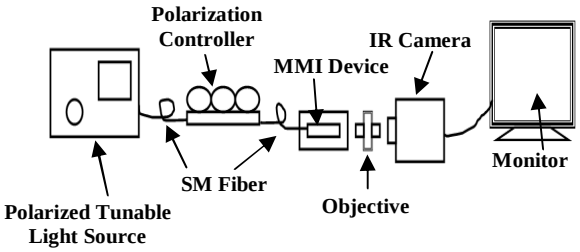

Fig. 5. A schematic diagram of characterization setup.

The result of the fiber scanning measurement is shown in Fig. 6. The effective refractive index, n_{eff} for the sample was 1.4457 and the wavelength of the laser was selected to be 1634.68 nm. This was the optimal wavelength to yield a clean three spot pattern for the actual physical length of the device and therefore produced the cleanest mode profile at the output facet and tallied with the simulation results. The launched power into the sample was 0.8 mW and it has been observed that the total output power from the three spots beam was 0.41 mW. This corresponds to around -3dB insertion losses which is a combination of the scattering loss due to the roughness of the MMI surface and modal mismatch.

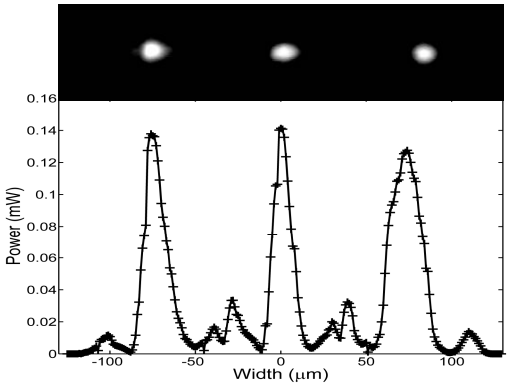

Fig. 6. Measured mode profile at the output facet of the 1 x 3 MMI splitter device without any refractive index oil in the trenches. Above shows the modal image recorded by the NIR camera, below is the measurement from the scanned fiber.

It has been observed that there were other small peaks in addition to the three predicted peaks in the mode profile images. This is probably because the thickness of the core layer is not quite optimal and can support some higher order modes at this wavelength. It can be observed from the NIR camera that the output spots were not ideally round in shape indicating some modal mismatch to the single mode fiber. However, we anticipate that by fabricating flat-fibers with smaller core dimensions it should be possible to avoid that problem. To demonstrate an additional feature of the use of micromachined trenches, we placed refractive index oil (n=1.44) within the trenches. We observed that the image at the output facet was changed to six peaks with different intensity levels as depicted in Fig. 7. This is because the different index contrast between the core layer and the refractive index oil has affected the width of the MMI region and changed the mode profile at the output facet. From this observation, we suggest that MMI flat-fiber devices can be potentially used as a refractive index sensor or be tuned for specific modal control.

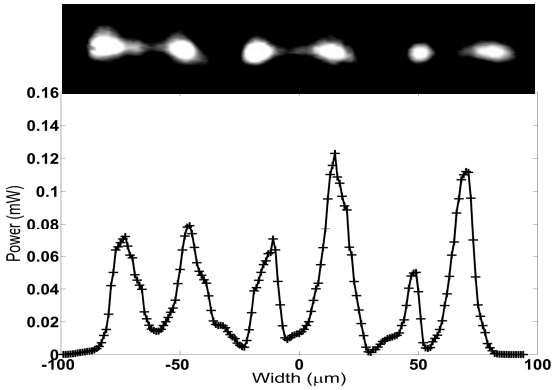

Fig. 7. Measured mode profile at the output facet of 1 x 3 MMI splitter device after adding the 1.44 refractive index oil. Above shows the modal image recorded by the NIR camera, below is the measurement from the scanned fiber.

IV. CONCLUSIONS

We have demonstrated a 1x3 MMI splitter device using a novel flat-fiber exhibiting around – 3dB insertion loss. The device was fabricated using a precision micromachining approach and makes use of micromachined trenches which allows for tuning of the device outputs by adding index fluids. The device operation matches closely with BPM modeling of the structure. This basic MMI splitter will be further explored to produce more sophisticated tunable devices in the future.

ACKNOWLEDGMENT

This research was funded by EPSRC, United Kingdom and University Technology of Malaysia, Malaysia.

REFERENCES

[1] L. B. Soldano and E. C. M. Pennings, "Optical multi-mode interference devices based on self-imaging: Principles and applications," *Journal Lightwave Technology*, vol. 13, no.4, pp. 615 – 627, Apr. 1995.

[2] C. J. Kaalund and Z. Jin, "Novel multimode interference devices for low index contrast materials systems featuring deeply etched air trenches", *Optics Communication*, 292-296 (2005).

[3] Q. Wang, G. Farrell and W. Yan, "Investigation on single-mode-

multimode-single-mode fiber structure", *Journal Lightwave Technology*, vol. 26, no. 5, March 2008.

[4] T. Liu, A. R. Zakharian, M. Fallahi, J. V. Moloney, and M. Mansuripur, "Multimode interference-based photonic crystal waveguide power splitter", *Journal of Lightwave Technology*, vol. 22, issue12, pp. 2842, 2004.

[5] C. Holmes, H. E. Major, J. C. Gates, C. B. E. Gawith, and P.G. R. Smith, "Period adapted Bragg mirror multimode interference device", *Conference on Lasers and Electro-optics/Quantum Electronics and Laser Science Conference (CLEO/QELS)*, vol. 1 -5, page 2865-2866, 2009.

[6] J. H. Kim, B. W. Dudley, and P. J. Moyer, "Experimental demonstration of replicated multimode interferometer power splitter in Zr-doped sol-gel", *Journal of Lightwave Technology*, vol. 24, issue. 1, page 612, 2006.

[7] M. H. Ibrahim, N. M. Kassim, A. B. Mohammad, M. K. Chin and S. Y. Lee, "Polymeric Optical Splitter Based on Multimode Interference Mechanism", *4th Student conference on Research and Development (SCOReD)*, Malaysia, IEEE, (2006).

[8] A. S. Webb, F. R. Mahamd Adikan, J. K. Sahu, R. J. Standish, C. B. E. Gawith, J. C. Gates, P. G. R. Smith and D. N. Payne, " MCVD planar substrates for UV-written waveguide devices", *Electronics Letters*, Vol .43(9), (2007)

[9] Katsunari Okamoto, "Fundamental of Optical Waveguides", *Academic Press* (2006).